Tetrahedron 67 (2011) 7231–7235

Contents lists available at ScienceDirect

Tetrahedron

journal homepage: www.elsevier.com/locate/tet

A tetrathiafulvalene-functionalized naphthalene diimide: synthesis, electrochemical and photophysical properties

Michael Jaggi [a], Belinda Schmid [a], Shi-Xia Liu [a,*], Sheshanath V. Bhosale [b,*], Shadi Rivadehi [b], Steven J. Langford [b], Silvio Decurtins [a]

[a] Departement für Chemie und Biochemie, Universität Bern, Freiestrasse 3, CH-3012 Bern, Switzerland
[b] School of Chemistry, Monash University Clayton, Vic-3800, Australia

ARTICLE INFO

Article history:
Received 1 July 2011
Accepted 21 July 2011
Available online 29 July 2011

Keywords:
Charge transfer
Donor–acceptor systems
Electrochemistry
Naphthalene diimide
Tetrathiafulvalene

ABSTRACT

A tetrathiafulvalene donor has been attached to the naphthalene diimide core via a rigid bridge affording a new planar molecular dyad. Its electronic properties have been studied experimentally by the combination of electrochemistry and UV–vis-NIR spectroscopy. Various electronic excited charge-transfer states are generated in different oxidation states, leading to almost full absorption in the visible to near-IR region with high extinction coefficients. The observed electronic properties are explained on the basis of density-functional-theory. In particular, the oxidized radical species show a strong tendency to undergo aggregation, in which the long-distance attractive interactions overcome the electrostatic repulsions.

1. Introduction

Core substituted naphthalene diimides (c-NDIs) have been rapidly emerging as an important class of molecules in the field of supramolecular and materials chemistry.[1] Whereas NDIs with hydrogen atoms on the naphthalene core have been used for a long time as electron acceptors in molecular dyads, their lack of absorbance in the visible region has prevented their use as chromophores.[1a] However, the addition of one or more substituents to the core of the naphthalene ring at the 2, 3, 6 or 7 position results in brightly coloured, conducting, functional materials with vastly different photophysical properties in comparison to those of the parent NDI.[2,3] This allows the whole visible region of the electromagnetic spectrum to be covered with a single series of chromophores that differ by a few atoms only. In parallel, a decrease of the energy of the longest wavelength electronic transition is observed upon increasing the number and the electron donating strength of the core substituents. As a consequence, these c-NDIs can be combined into arrays and supramolecular architectures that do not only operate as light harvesting antennas but also undergo charge separation and charge conduction; altogether these are unique properties relevant to the fields of artificial photosynthesis and photovoltaics.[4]

Tetrathiafulvalene (TTF) represents one of the most intensively investigated redox-active organic molecules due to its intrinsic properties, namely two easily accessible oxidized states ($TTF^{\bullet+}$ and TTF^{2+}), which display distinctly different physical properties.[5] By the appropriate functionalization, a variety of TTF-incorporating systems find applications in diverse fields, such as redox-controllable molecular machines, biological probes, switches, liquid crystals, gels, organic field-effect transistors and solar cells.[6] Among them, TTF derivatives, as electron-donor units in donor–acceptor (D–A) ensembles, are of prime interest in molecular (opto)electronics. In response, we have introduced a concept for the annulation of TTFs to acceptor moieties via a Schiff-base reaction, leading to various sterically controlled and compactly fused D–π-A systems. They show pronounced photoinduced charge-transfer (CT) processes giving rise to interesting photophysical phenomena, such as long-lived charge-separated states and/or they bear small HOMO–LUMO gaps.[7–8] In contrast to these earlier studies, which mainly have a focus on the pyrazine bridging unit, the herein reported c-NDI–TTF dyad **1** results from the incorporation of TTF to the NDI core via a rigid diaza bridge (Fig. 1). Thereby, in much the same way as it was deduced from the single crystal structure determination of c-NDI–Ts (Fig. 1),[3c] the actual dyad **1** is expected to have a structurally rigid and planar conformation. Very recently, an analogous D–A system but with a porphyrin rather than a TTF unit as an electron donor has been reported; recognizably it exhibits a substantial electronic coupling between the individual units (c-NDI and porphyrin).[3e] As the focal

* Corresponding authors. Tel.: +41 31 631 4296; fax: +41 31 631 4399 (S.-X.L.); tel.: +61 3 9905 5980; fax: +61 3 9905 4597 (S.V.B.); e-mail addresses: liu@iac.unibe.ch (S.-X. Liu), sheshanath.bhosale@monash.edu (S.V. Bhosale).

0040-4020/$ – see front matter © 2011 Elsevier Ltd. All rights reserved.
doi:10.1016/j.tet.2011.07.069

point of the present work, we explore the electrochemical and photophysical properties of **1** and demonstrate the combination of a pronounced redox behaviour and a strong photoinduced intramolecular charge-transfer (ICT) process within this new molecular dyad.

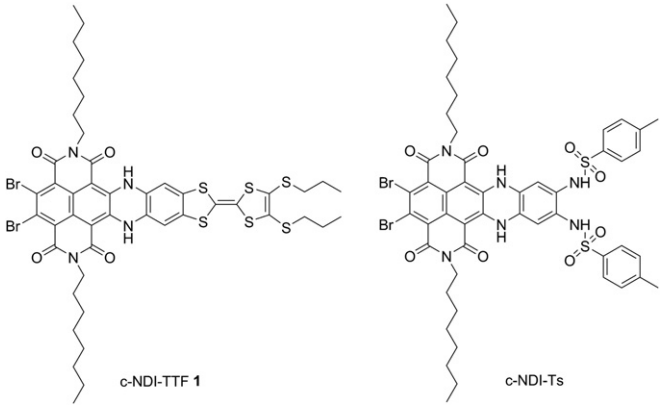

Fig. 1. Chemical structures of the c-NDI–TTF dyad **1** and the reference compound c-NDI–Ts.

2. Results and discussion

In brief, c-NDI–TTF dyad **1** was synthesized as a dark green crystalline solid in 94% yield by the condensation of the tetrabromo-NDI **2** with diamino-TTF **3** under argon atmosphere in dry DMF at 135 °C (Scheme 1). According to the literature procedures, compound **2** was prepared from naphthalene dianhydride in two steps[9,10] while compound **3** was obtained as a yellow powder in 35% yield via a phosphite-mediated self-coupling reaction of 5,6-diamino-1,3-benzodithiole-2-thione with 4,5-bis(propylthio)-1,3-dithiole-2-one.[7d]

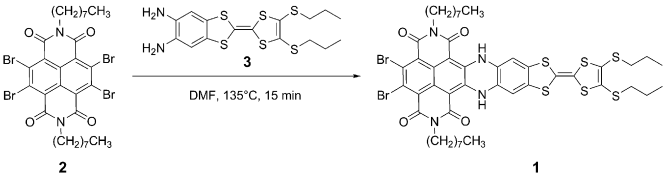

Scheme 1. Synthesis of c-NDI–TTF dyad **1**.

The electrochemical properties of the dyad **1** and the reference compound c-NDI–Ts in CH_2Cl_2 were investigated by cyclic voltammetry. c-NDI–TTF **1** undergoes three reversible oxidations ($E^{ox1}_{1/2}$ =0.58 V, $E^{ox2}_{1/2}$=0.91 V and $E^{ox3}_{1/2}$=1.49 V), which can be assigned to the consecutive oxidations of the TTF core to the radical and dication species, followed by the oxidation of the linker, 1,4-dihydropyrazine (Fig. 2, black line). The first two oxidation potentials are anodically shifted compared to those of compound **3** ($E^{ox1}_{1/2}$=0.36 V and $E_{1/2}{}^{ox2}$=0.73 V)[7d] due to an electron-withdrawing effect of the NDI group. Similarly, the third oxidation process is anodically shifted by comparison with that of c-NDI–Ts, which appears irreversible as evidenced by the presence of one anodic peak at E_{pa}=1.05 V and two related cathodic peaks at E^1_{pc}=0.93 V and E^2_{pc}=0.76 V. This observation is not unexpected on the basis of simple electrostatic arguments; the TTF unit is oxidized first in the c-NDI–TTF dyad **1**.

In order to describe and analyze the electronic transitions of dyad **1**, it is advantageous to apply a symmetry frame to the molecule. In the following, the discussion is based on the C_{2v} point group symmetry, and consequently one of the mirror planes allows for a strict σ–π separation of the electronic structure of the π-conjugated molecule. The overall good agreement of the calculated results with

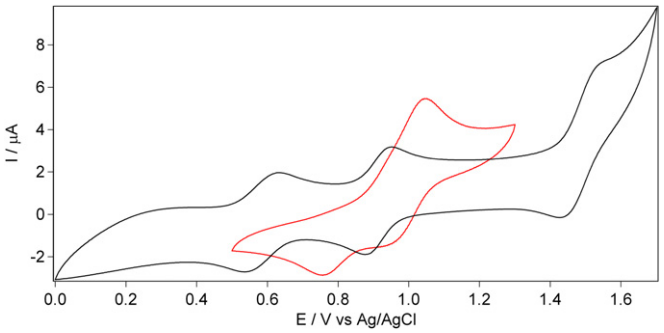

Fig. 2. Cyclic voltammograms of **1** (black line, 4.45×10^{-4} M) and the reference compound c-NDI–Ts (red line, 3.74×10^{-4} M) in CH_2Cl_2; 0.1 M $TBAPF_6$; on platinum electrode at 200 mV/s.

the experimental ones justifies this approach; the calculated symmetry-allowed in-plane electric dipole transitions match the electronic spectrum fairly well. The molecular orbitals (MOs) with their calculated energies that are dominantly involved in the more intense electronic transitions are given in Fig. 3. They all reflect a B_1 symmetry (the molecule lies in the plane of the *yz* coordinates) and thus the symmetry-allowed electronic dipole transitions are polarized along the long molecular axis. The electron densities of the highest occupied MO (HOMO) and the lowest unoccupied MO (LUMO) are mostly localized on the TTF and c-NDI part, respectively, however in each case some extension into the bridging area occurs; evidently, this will lead to an appreciable orbital overlap with respect to the transition dipole moment for an HOMO to LUMO transition. The HOMO−1 is delocalized over the whole molecule and the LUMO+8 corresponds to a LUMO of TTF itself. The calculated HOMO–LUMO gap results in a value of 1.66 eV (13,400 cm^{-1}), which compares favourably with the onset of the first absorption band of the optical spectrum of **1**. Similarly, Fig. 4 shows the relevant MOs that are dominantly involved in the more intense electronic transitions of the reference compound c-NDI–Ts, however, the calculation is restricted to the core fragment of this reference molecule. Not surprisingly, its HOMO and LUMO are strongly related to the HOMO−1 and LUMO of **1**. The calculated HOMO–LUMO gap results in a value of 2.43 eV (19,600 cm^{-1}), which only roughly approximates the first absorption band of the optical spectrum of c-NDI–Ts.

The dark green compound **1** shows intense optical absorption bands over an extended range within the UV–vis spectral region (Fig. 5). The electronic transitions can best be characterized in terms of three distinct energy ranges. Firstly, at low energy, a single strong absorption band appears at 15,000 cm^{-1} (667 nm), which can be attributed to an intramolecular TTF→c-NDI charge-transfer (ICT) transition (see below) similar to that in the previously reported c-NDI–porphyrin dyad.[3e] Secondly, three absorption bands appear at 16,490 cm^{-1} (606 nm), 17,840 cm^{-1} (560 nm) and 19,190 cm^{-1} (521 nm) showing an intensity profile, which originates from an electronic transition at 16,490 cm^{-1} with a clear progression in a 1350 cm^{-1} vibrational mode. Thirdly, in the high energy range above 25,000 cm^{-1} (400 nm) characteristic π–π* transitions of the TTF and c-NDI chromophores appear. By comparison with the spectrum of the blue coloured c-NDI–Ts compound it seems clear that the lowest energy absorption band of **1**, at 15,000 cm^{-1} (667 nm), is specifically characteristic of the D–A dyad. Interestingly, the second electronic transition with its vibrational progression is energetically not shifted through the linkage of the TTF unit.

The calculated vertical electronic transitions for c-NDI–TTF (**1**) and the core fragment of c-NDI–Ts are shown by stick spectra in Fig. 6, and the calculated energy values and oscillator strengths of both compounds are given in Table 1.

For **1**, the TD–DFT calculation predicts the $S_0\rightarrow S_1$ excitation to be dominated (99%) by a one-electron HOMO→LUMO promotion and

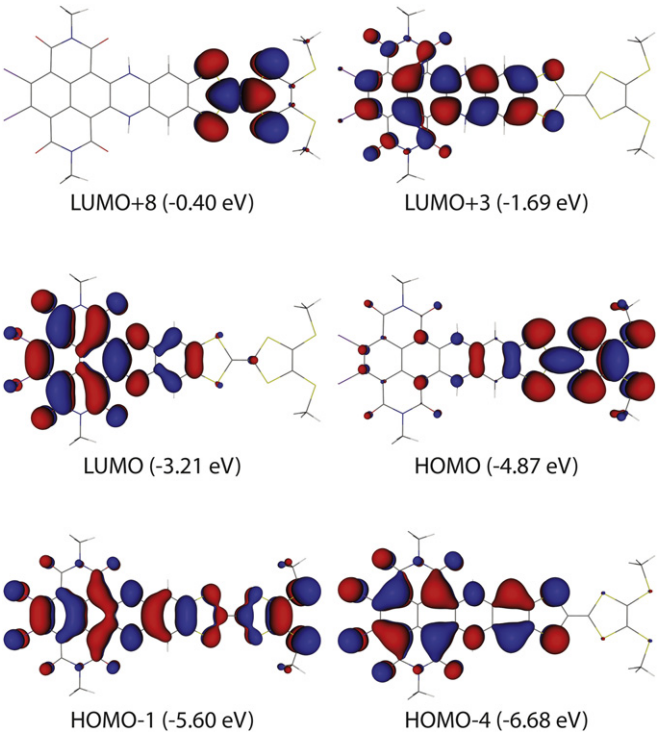

Fig. 3. Molecular orbitals of c-NDI–TTF **1** (with methyl instead of propyl and octyl groups).

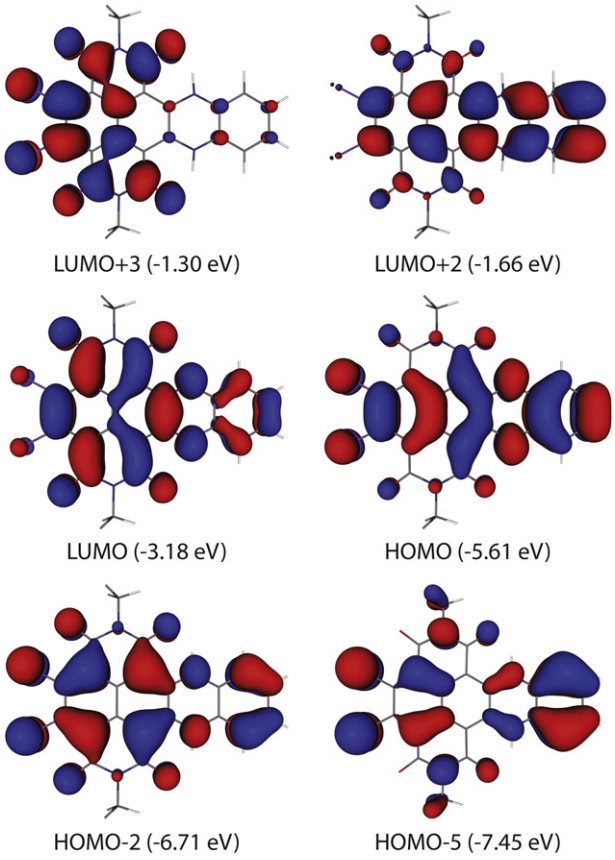

Fig. 4. Molecular orbitals of the core fragment of c-NDI–Ts (with methyl instead of octyl groups).

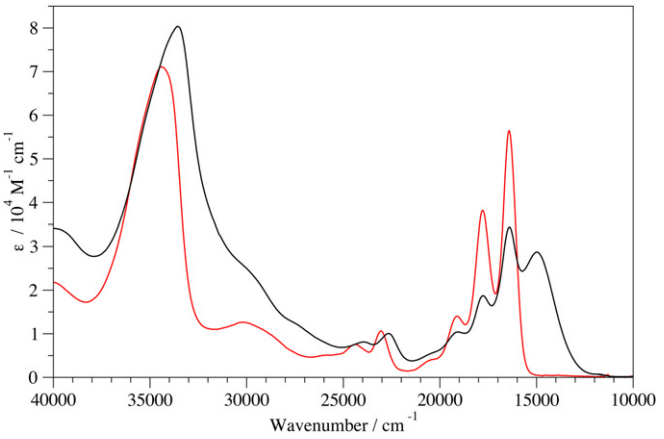

Fig. 5. Electronic absorption spectrum of c-NDI–TTF dyad **1** (black line) together with that of the reference compound c-NDI–Ts (red line) in CH_2Cl_2 solutions.

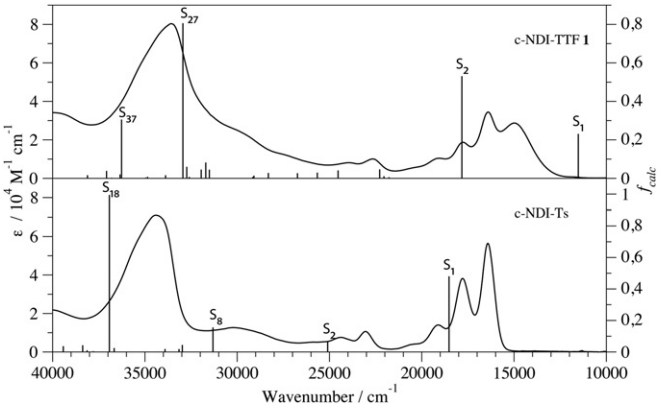

Fig. 6. Electronic absorption spectra of c-NDI–TTF dyad **1** (top) and of the reference compound c-NDI–Ts (bottom) together with the calculated $S_0 \rightarrow S_n$ transitions at the TD-B3LYP/TZVP level of theory.

Table 1
Values of energies, oscillator strengths and dominant contributions of the respective molecular orbitals for $S_0 \rightarrow S_n$ transitions of **1** and the core fragment of c-NDI–Ts

Compound	State	Excitation energy (cm^{-1})	Oscillator strength	Dominant contribution (%)
Dyad **1**	S_1	11,520	0.23	H→L (99)
	S_2	17,826	0.53	H−1→L (98)
	S_{27}	32,940	0.81	H→L+8 (86)
	S_{37}	36,264	0.31	H−4→L+3 (83)
The core fragment of c-NDI–Ts	S_1	18,523	0.48	H→L (97)
	S_2	25,099	0.06	H−2→L (87)
				H→L+2 (10)
	S_8	31,312	0.16	H→L+3 (76)
				H−5→L (15)
	S_{18}	36,925	0.99	H−2→L+2 (84)

thus exhibits pronounced charge-transfer character since electron density is moved from the TTF moiety to the c-NDI part. In view of this substantial charge flow across the molecular backbone, the calculated energy and oscillator strength compare fairly well with the first single absorption band centred at 15,000 cm^{-1} (667 nm). Next, the calculated $S_0 \rightarrow S_2$ excitation is dominated (98%) by a one-electron HOMO−1→LUMO promotion. Its main character is reflected by a π–π* transition within the c-NDI moiety (although with some extension into the bridging area). At higher energies, a manifold of less intense transitions follows, until with the $S_0 \rightarrow S_{27}$ and $S_0 \rightarrow S_{37}$ excitations strong π–π* transitions within the TTF and c-NDI units appear. Similarly, the calculated vertical electronic transitions for the core

fragment of c-NDI–Ts match well with the experimental absorption spectrum of c-NDI–Ts. Noteworthy, the $S_0 \rightarrow S_1$ excitation, dominated (97%) by a one-electron HOMO→LUMO promotion, bears its striking analogy to the HOMO−1→LUMO promotion of **1**, a result, which is experimentally expressed by the similarity of the optical spectra of both compounds in the respective energy range.

Dyad **1** can be chemically oxidized to its radical cation $\mathbf{1}^{\bullet+}$ by $FeCl_3$. Essentially, upon oxidation, a bleaching of the ICT band at 15,000 cm^{-1} (667 nm) and a concomitant gradual growth of new lower-energy absorption bands at 13,070 cm^{-1} (765 nm), 11,740 cm^{-1} (852 nm) and 7870 cm^{-1} (1270 nm) occur, as it is shown in Fig. 7. On the basis of previous observations,[7–8,11–13] these bands at 13,070 cm^{-1} (765 nm) and 11,740 cm^{-1} (852 nm) can be assigned to be characteristic of the cation radical species $\mathbf{1}^{\bullet+}$ and of another ICT transition, however in the opposite direction ($TTF^{\bullet+} \rightarrow$ c-NDI) to that of the neutral compound **1**. Particularly, the additional NIR absorption band at 7870 cm^{-1} (1270 nm) is presumably attributed to the aggregation of radical cation species $\mathbf{1}^{\bullet+}$ arising from the strong π–π interactions stabilized by its planar conformation via intramolecular hydrogen bonds. It can therefore be deduced that $\mathbf{1}^{\bullet+}$ shows a strong tendency to undergo aggregation, in which the long-distance attractive interaction overcomes the electrostatic repulsion. The direct observation of such strong aggregation in diluted solution at room temperature is still quite challenging because the intermolecular interactions are usually too weak to associate the $TTF^{\bullet+}$ units noncovalently.

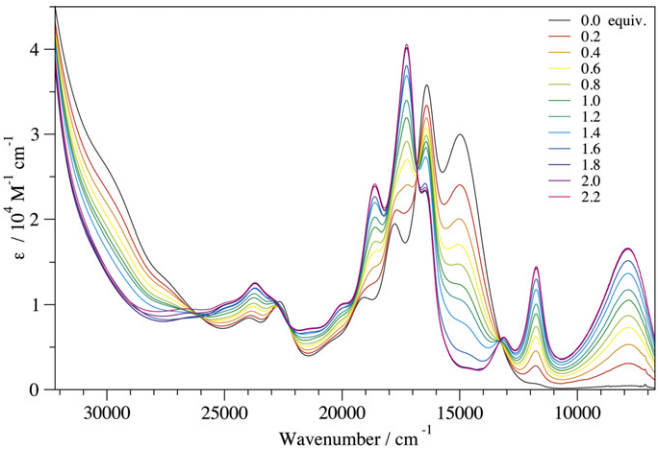

Fig. 7. Variation of the UV–vis-NIR absorption spectra of **1** (2.25×10^{-5} M) in CH_2Cl_2 upon successive addition of aliquots of $FeCl_3$.

3. Conclusion

In conclusion, a first example of the incorporation of TTF to the c-NDI molecule via a rigid diaza bridge has been reported. For this redox-active D–A dyad, a strong electronic absorption profile extends far into the visible spectral region, which originates from its inherent electronic donor-acceptor nature. By virtue of its rigid and planar structural feature, significant π–π interactions were observed, corroborated by the presence of a strong absorption at 7870 cm^{-1} (1270 nm) upon chemical oxidation. Specifically, molecular systems having two or more redox-active centres in close proximity, capable of cooperative interactions, are of prime interest in the development of molecular electronics.

4. Experimental section

4.1. Equipment

^1H and ^{13}C NMR spectra were recorded on a Bruker spectrometer using $CDCl_3$ as solvent and tetramethylsilane as an internal standard. The following abbreviations were used s (singlet), d (doublet), t (triplet) and m (multiplet). Elemental analyses were performed on a Perkin–Elmer 2400 LSII CHN analyzer. HRMS data were obtained with a Sciex QSTAR Pulsar mass spectrometer for ESI (electrospray ionization) mode. IR spectra were recorded on a Perkin–Elmer Spectrum One FT-IR spectrometer and are reported as wave numbers ν in cm^{-1} with band intensities indicated as s (strong), m (medium), w (weak). UV–vis absorption spectra of **1** and c-NDI–Ts in CH_2Cl_2 were recorded on a Perkin–Elmer Lambda 10 spectrometer at room temperature. Concerning the evolution of UV–vis-NIR spectra of **1** after successive addition of $FeCl_3$ aliquots, the experiments were carried out on a Perkin–Elmer Lambda 900 spectrometer in a 1 cm quartz cell using a solution of **1** (2.25×10^{-5} M) in CH_2Cl_2 and a solution of $FeCl_3$ (4.5×10^{-3} M) in CH_3CN.

4.2. Electrochemistry

Dichloromethane (HPLC grade, Acros) and tetra-*n*-butylammonium hexafluorophosphate ($TBAPF_6$, electrochemical grade, Fluka) were used as received.

Cyclic voltammetry was performed in a three-electrode cell equipped with a Pt disk working electrode, a glassy carbon counter-electrode, and Ag/AgCl was used as reference electrode. The electrochemical experiments were carried out under dry and O_2-free atmosphere in dichloromethane with $Bu_4N(PF_6)$ (0.1 M) as support electrolyte. The voltammograms were recorded on a PGSTAT 101 potentiostat.

4.3. Computational methods

For ab initio calculations, density-functional-theory (DFT) and time-dependent DFT methods were performed with the B3LYP hybrid functional and the TZVP basis set. All calculations were carried out with the TURBOMOLE V6.0 program package.[14] The molecular ground state geometries were optimized at the B3LYP/TZVP level of theory and constrained to have C_{2v} symmetry. The electronic excitation spectra were calculated with the larger TZVP basis set.

4.4. Materials

Unless otherwise stated, all reagents were purchased from Aldrich and used without additional purification. The solvents for spectroscopic studies were of spectroscopic grade and used as received. 2,3,6,7-Tetrabromo-dioctyl-naphthalene diimide[9,10] and 5,6-diamino-2-(4,5-bis(propylthio)-1,3-dithio-2-ylidene)benzo[*d*][1,3]dithiole[7d] were prepared following the literature procedures. Air- and/or water-sensitive reactions were conducted under argon using dry solvents.

*4.4.1. 12-(4,5-Bis(propylthio)-1,3-dithiol-2-ylidene)-4,5-dibromo-2-ethyl-7-octyl-[1,3]dithiolo[4,5-i][3,8]phenanthrolino[1,10-abc]phenazine-1,3,6,8(2H,7H,9H,15H)-tetraone (c-NDI–TTF) (**1**).* A mixture of 2,3,6,7-tetrabromo-dioctyl-naphthalene diimide **2** (100 mg, 0.124 mmol) and 5,6-diamino-2-(4,5-bis(propylthio)-1,3-dithio-2-ylidene)-benzo[*d*][1,3]dithiole **3** (0.0535 mg, 0.124 mmol) in dry DMF (5 mL) was heated at 135 °C for 15 min (colour change was observed from yellowish to dark green). Completion of the reaction was monitored by TLC. After completion DMF was removed on rotary evaporator, and the residue was purified by column chromatography on flash silica column (100:1 CH_2Cl_2/CH_3OH) to give the *title compound* **1** (125 mg, 94%) as a dark green crystalline powder. IR (KBr, cm^{-1}): 3392, 3320, 2959, 2925, 2852, 1716, 1666, 1502, 1489, 1431, 1374, 1287, 1173, 1157, 1013, 910, 789, 854. ^1H NMR ($CDCl_3$, 300 MHz) δ: 13.01 (s, 2H, core-NH), 6.55 (s, 2H), 4.11–4.06

(t, J=8.0 Hz, 4H), 2.78–2.73 (t, J=6.4 Hz, 4H), 1.68–1.63 (m, 4H), 1.61–1.52 (m, 4H), 1.39–1.25 (m, 20), 1.03–0.98 (t, J=6.8 Hz, 6H), 0.90–0.88 (t, J=7.2 Hz, 6H). ^{13}C NMR ($CDCl_3$, 125 MHz) δ: 164.4, 159.9, 140.94, 135.07, 128.3, 127.5, 126.9, 121.4, 114.3, 108.8, 41.3, 36.2, 21.8, 29.7, 29.3, 27.8, 27.3, 23.1, 22.6, 14.1, 13.1; HRMS (ESI): calcd for $C_{46}H_{52}Br_2N_4O_4S_6$ 1077.1275; found 1077.1180. Anal. Calcd for $C_{46}H_{52}Br_2N_4O_4S_6$: C 51.29, H 4.87, N 5.20; found C 51.56, H 4.88, N 5.13.

Acknowledgements

This work was supported by the Swiss National Science Foundation (grant No. 200020–130266/1). S.V.B. and S.J.L. gratefully acknowledge the Australian Research Council for support under the Discovery program (DP0878220 and DP0878756). S.V.B. thanks A.R.C. for A.P.D. fellowship. We also thank Yasushi Morita for providing compound **3**.

Supplementary data

Supplementary data associated with this article can be found in the online version, at doi:10.1016/j.tet.2011.07.069. These data include MOL files and InChIKeys of the most important compounds described in this article.

References and notes

1. (a) Bhosale, S.; Jani, C.; Langford, S. J. *Chem. Soc. Rev.* **2008**, *37*, 331; (b) Bhosale, R.; Misek, J.; Sakai, N.; Matile, S. *Chem. Soc. Rev.* **2010**, *39*, 138; (c) Pan, M.; Lin, X.-M.; Li, G.-B.; Su, C.-Y. *Coord. Chem. Rev.* **2011**, *255*, 1921.
2. Würthner, F.; Ahmed, S.; Thalacker, C.; Debaerdemaeker, T. *Chem.—Eur. J.* **2002**, *8*, 4742.
3. (a) Sakai, N.; Mareda, J.; Vauthey, E.; Matile, S. *Chem. Commun.* **2010**, 4225; (b) Bhosale, S. V.; Jani, C.; Lalander, C. H.; Langford, S. J. *Chem. Commun.* **2010**, 973; (c) Bhosale, S. V.; Bhosale, S. V.; Kalyankar, M. B.; Langford, S. J. *Org. Lett.* **2009**, *11*, 5418; (d) Bhosale, S. V.; Kalyankar, M. B.; Bhosale, S. V.; Langford, S. J.; Reid, E. F.; Hogan, C. F. *New J. Chem.* **2009**, *33*, 2409; (e) Bajerji, N.; Bhosale, S. V.; Petkova, I.; Langford, S. J.; Vauthey, E. *Phys. Chem. Chem. Phys.* **2011**, *13*, 1019.
4. Bhosale, S.; Sisson, A.; Talukdar, P.; Fürstenberg, A.; Banerj, N.; Vauthey, E.; Bollot, S.; Mareda, J.; Röger, C.; Würthner, F.; Sakai, N.; Matile, S. *Science* **2006**, *313*, 84.
5. (a) Segura, J. L.; Martín, N. *Angew. Chem., Int. Ed.* **2001**, *40*, 1372; (b) Lorcy, D.; Bellec, N.; Fourmigué, M.; Avarvari, N. *Coord. Chem. Rev.* **2009**, *253*, 1398; (c) Canevet, D.; Sallé, M.; Zhang, G.; Zhang, D.; Zhu, D. *Chem. Commun.* **2009**, 2245.
6. (a) Li, X.; Zhang, G.; Ma, H.; Zhang, D.; Li, J.; Zhu, D. *J. Am. Chem. Soc.* **2004**, *126*, 11543; (b) Loosli, C.; Jia, C. Y.; Liu, S.-X.; Haas, M.; Dias, M.; Levillain, E.; Neels, A.; Labat, G.; Hauser, A.; Decurtins, S. *J. Org. Chem.* **2005**, *70*, 4988; (c) Yasuda, T.; Tanabe, K.; Tsuji, T.; Cotí, K. K.; Aprahamian, I.; Stoddart, J. F.; Kato, T. *Chem. Commun.* **2010**, 1224; (d) Bigot, J.; Charleux, B.; Cooke, G.; Delattre, F.; Fournier, D.; Lyskawa, J.; Sambe, L.; Stoffelbach, F.; Woisel, P. *J. Am. Chem. Soc.* **2010**, *132*, 10796; (e) Wu, J.-C.; Liu, S.-X.; Neels, A.; Le Derf, F.; Sallé, M.; Decurtins, S. *Tetrahedron* **2007**, *63*, 11282; (f) Wu, J.-C.; Dupont, N.; Liu, S.-X.; Neels, A.; Hauser, A.; Decurtins, S. *Chem.—Asian J.* **2009**, *4*, 392; (g) Delahaye, S.; Loosli, C.; Liu, S.-X.; Decurtins, S.; Labat, G.; Neels, A.; Loosli, A.; Ward, T. R.; Hauser, A. *Adv. Funct. Mater.* **2006**, *16*, 286.
7. (a) Jia, H.-P.; Liu, S.-X.; Sanguinet, L.; Levillain, E.; Decurtins, S. *J. Org. Chem.* **2009**, *74*, 5727; (b) Guégano, X.; Kanibolotsky, A. L.; Blum, C.; Mertens, S. F. L.; Liu, S.-X.; Neels, A.; Hagemann, H.; Skabara, P. J.; Leutwyler, S.; Wandlowski, T.; Hauser, A.; Decurtins, S. *Chem.—Eur. J.* **2009**, *15*, 63; (c) Wu, J.-C.; Liu, S.-X.; Keene, T. D.; Neels, A.; Mereacre, V.; Powell, A. K.; Decurtins, S. *Inorg. Chem.* **2008**, *47*, 3452; (d) Jia, C.-Y.; Liu, S.-X.; Tanner, C.; Leiggener, C.; Neels, A.; Sanguinet, L.; Levillain, E.; Leutwyler, S.; Hauser, A.; Decurtins, S. *Chem.—Eur. J.* **2007**, *13*, 3804; (e) Jia, C.-Y.; Liu, S.-X.; Tanner, C.; Leiggener, C.; Sanguinet, L.; Levillain, E.; Leutwyler, S.; Hauser, A.; Decurtins, S. *Chem. Commun.* **2006**, 1878; (f) El-Khouly, M. E.; Jaggi, M.; Schmid, B.; Blum, C.; Liu, S.-X.; Decurtins, S.; Ohkubo, K.; Fukuzumi, S. *J. Phys. Chem. C* **2011**, *115*, 8325.
8. (a) Jaggi, M.; Blum, C.; Dupont, N.; Grilj, J.; Liu, S.-X.; Hauser, J.; Hauser, A.; Decurtins, S. *Org. Lett.* **2009**, *11*, 3096; (b) Jaggi, M.; Blum, C.; Marti, B. S.; Liu, S.-X.; Leutwyler, S.; Decurtins, S. *Org. Lett.* **2010**, *12*, 1344; (c) Goze, C.; Leiggener, C.; Liu, S.-X.; Sanguinet, L.; Levillain, E.; Hauser, A.; Decurtins, S. *Chem. Phys. Chem.* **2007**, *8*, 1504; (d) Goze, C.; Dupont, N.; Beitler, E.; Leiggener, C.; Jia, H.; Monbaron, P.; Liu, S.-X.; Neels, A.; Hauser, A.; Decurtins, S. *Inorg. Chem.* **2008**, *47*, 11010; (e) Ran, Y.-F.; Blum, C.; Liu, S.-X.; Sanguinet, L.; Levillain, E.; Decurtins, S. *Tetrahedron* **2011**, *67*, 1623; (f) Dupont, N.; Ran, Y.-F.; Jia, H.-P.; Grilj, J.; Ding, J.; Liu, S.-X.; Decurtins, S.; Hauser, A. *Inorg. Chem.* **2011**, *50*, 3295.
9. Gao, X.; Qiu, W.; Yang, X.; Liu, Y.; Wang, Y.; Zhang, H.; Qi, T.; Liu, Y.; Lu, K.; Du, C.; Shuai, Z.; Yu, G.; Zhu, D. *Org. Lett.* **2007**, *9*, 3917.
10. Tahara, K.; Furukawa, S.; Uji, H.; Uchino, T.; Ichikawa, T.; Zhang, J.; Mamdouh, W.; Sonoda, M.; De Schryver, F. C.; De Feyter, S.; Tobe, Y. *J. Am. Chem. Soc.* **2006**, *128*, 16613.
11. (a) Li, H.; Lambert, C. *Chem.—Eur. J.* **2006**, *12*, 1144; (b) Nakamura, K.; Takashima, T.; Shirahata, T.; Hino, S.; Hasegawa, M.; Mazaki, Y.; Misaki, Y. *Org. Lett.* **2011**, *13*, 3122.
12. (a) Chiang, P.-T.; Chen, N.-C.; Lai, C.-C.; Chiu, S.-H. *Chem.—Eur. J.* **2008**, *14*, 6546; (b) Kitahara, T.; Shirakawa, M.; Kawano, S.-I.; Beginn, U.; Fujita, N.; Shinkai, S. *J. Am. Chem. Soc.* **2005**, *127*, 14980; (c) Ziganshina, A. Y.; Ko, Y. H.; Jeon, W. S.; Kim, K. *Chem. Commun.* **2004**, 806; (d) Yoshizawa, M.; Kumazawa, K.; Fujita, M. *J. Am. Chem. Soc.* **2005**, *127*, 13456; (e) Rosokha, S. V.; Kochi, J. K. *J. Am. Chem. Soc.* **2007**, *129*, 828.
13. (a) Barin, G.; Coskun, A.; Friedman, D. C.; Olson, M. A.; Colvin, M. T.; Carmielli, R.; Dey, S. K.; Bozdemir, O. A.; Wasielewski, M. R.; Stoddart, J. F. *Chem.—Eur. J.* **2011**, *17*, 213; (b) Aprahamian, I.; Olsen, J.-C.; Trabolsi, A.; Stoddart, J. F. *Chem.—Eur. J.* **2008**, *14*, 3889; (c) Spruell, J. M.; Coskun, A.; Friedman, D. C.; Forgan, R. S.; Sarjeant, A. A.; Trabolsi, A.; Fahrenbach, A. C.; Barin, G.; Paxton, W. F.; Dey, S. K.; Olson, M. A.; Benítez, D.; Tkatchouk, E.; Colvin, M. T.; Carmielli, R.; Caldwell, S. T.; Rosair, G. M.; Hewage, S. G.; Duclairoir, F.; Seymour, J. L.; Slawin, A. M. Z.; Goddard, W. A., III; Wasielewski, M. R.; Cooke, G.; Stoddart, J. F. *Nat. Chem.* **2010**, *2*, 870; (d) Coskun, A.; Spruell, J. M.; Barin, G.; Fahrenbach, A. C.; Forgan, R. S.; Colvin, M. T.; Carmieli, R.; Benítez, D.; Tkatchouk, E.; Friedman, D. C.; Sarjeant, A. A.; Wasielewski, M. R.; Goddard, W. A., III; Stoddart, J. F. *J. Am. Chem. Soc.* **2011**, *133*, 4538.
14. (a) Treutler, O.; Ahlrichs, R. *J. Chem. Phys.* **1995**, *102*, 346; (b) Hättig, C.; Weigend, F. *J. Chem. Phys.* **2000**, *113*, 5154; (c) Hättig, C.; Köhn, A. *J. Chem. Phys.* **2002**, *117*, 6939.